

## An earth-isolated optically coupled wideband high voltage probe powered by ambient light

Xiang Zhai and Paul M. Bellan

Citation: *Rev. Sci. Instrum.* **83**, 104703 (2012); doi: 10.1063/1.4757112

View online: <http://dx.doi.org/10.1063/1.4757112>

View Table of Contents: <http://rsi.aip.org/resource/1/RSINAK/v83/i10>

Published by the [American Institute of Physics](#).

---

### Related Articles

Reduction in subsidy for solar power as distributed electricity generation in Indian future competitive power market

[J. Renewable Sustainable Energy 4, 053120 \(2012\)](#)

Optimized working conditions for a thermoelectric generator as a topping cycle for gas turbines

[J. Appl. Phys. 112, 073515 \(2012\)](#)

Determination of salinity gradient power potential in Québec, Canada

[J. Renewable Sustainable Energy 4, 053113 \(2012\)](#)

Case study: Simulation and optimization of photovoltaic-wind-battery hybrid energy system in Taleghan-Iran using homer software

[J. Renewable Sustainable Energy 4, 053111 \(2012\)](#)

Feasibility study in application of forging waste heat on absorption cooling system

[J. Renewable Sustainable Energy 4, 053109 \(2012\)](#)

---

### Additional information on Rev. Sci. Instrum.

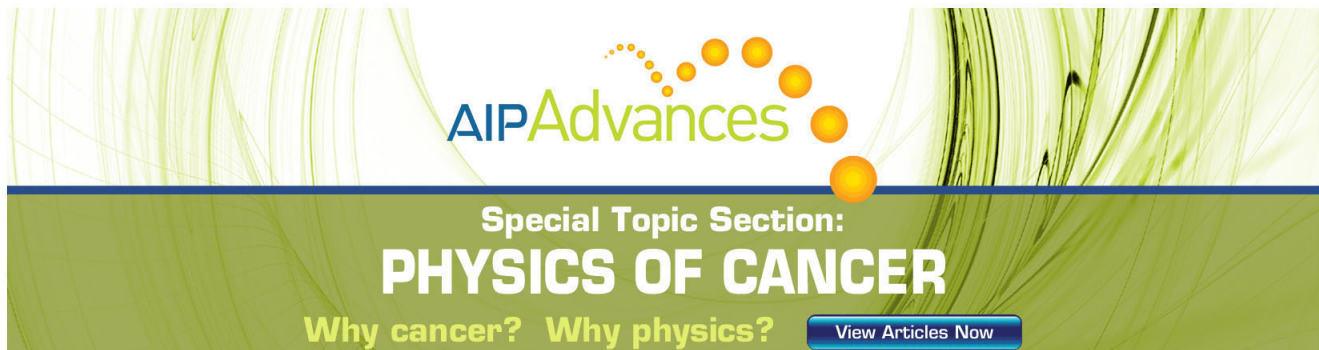
Journal Homepage: <http://rsi.aip.org>

Journal Information: [http://rsi.aip.org/about/about\\_the\\_journal](http://rsi.aip.org/about/about_the_journal)

Top downloads: [http://rsi.aip.org/features/most\\_downloaded](http://rsi.aip.org/features/most_downloaded)

Information for Authors: <http://rsi.aip.org/authors>

## ADVERTISEMENT



**AIP Advances**

Special Topic Section:  
**PHYSICS OF CANCER**

Why cancer? Why physics? [View Articles Now](#)

# An earth-isolated optically coupled wideband high voltage probe powered by ambient light

Xiang Zhai<sup>a)</sup> and Paul M. Bellan<sup>b)</sup>

*Thomas J. Watson Sr. Laboratories of Applied Physics, California Institute of Technology, Pasadena, California 91125, USA*

(Received 8 July 2012; accepted 17 September 2012; published online 9 October 2012)

An earth-isolated optically-coupled wideband high voltage probe has been developed for pulsed power applications. The probe uses a capacitive voltage divider coupled to a fast light-emitting diode that converts high voltage into an amplitude-modulated optical signal, which is then conveyed to a receiver via an optical fiber. A solar cell array, powered by ambient laboratory lighting, charges a capacitor that, when triggered, acts as a short-duration power supply for an on-board amplifier in the probe. The entire system has a noise level  $\leq 0.03$  kV, a DC-5 MHz bandwidth, and a measurement range from  $-6$  to 2 kV; this range can be conveniently adjusted. © 2012 American Institute of Physics. [<http://dx.doi.org/10.1063/1.4757112>]

## I. INTRODUCTION

Measuring rapidly changing high voltages in the presence of large currents is challenging because of substantial interference from ground loops, capacitive and inductive pickup, high frequency radiation, etc.

Various high voltage probes<sup>1-3</sup> and some commercial products (e.g., Tektronix P6015A) have been developed for measuring high voltage for different purposes. For example, a passive high voltage (HV) probe developed by Sarjeant and Alcock uses a resistive voltage divider and can measure a  $<100$  ns voltage pulse with subnanosecond rise time.<sup>1</sup> Another passive HV probe developed by Gratton *et al.* adopts a capacitive divider for measuring nanosecond HV pulses.<sup>2</sup> A capacitive-RC hybrid passive probe developed by Saw *et al.* is designed for fast pulse discharge systems.<sup>3</sup> However, most of these passive HV probes, including the Tektronix P6015A, require connection to earth ground, which makes them neither convenient for long distance measurements because of ground loop susceptibility, nor suitable for real floating voltage measurements. For example, the Caltech experimental plasma group uses a Tektronix P6015A probe for pulsed power voltage measurements. To isolate the data acquisition device from the HV source and to avoid long wires in an environment with fast changing magnetic fields, an optical link is used to convert the Tektronix probe voltage signals to optical signals near the HV source and then convert back to electrical signals for recording data. However, the optical link requires a power supply that plugs into the wall. Therefore, the Tektronix probe ground lead is electrically connected with mains ground through the optical link power supply, and hence cannot connect to the HV source ground. Otherwise, the entire system would have multiple points connected to earth ground and form ground loops, the latter can induce huge electromotive force (EMFs) in noisy environments, especially when a fast varying current exists close to the probe. With no ground lead connecting to the HV source,

the Tektronix probe is actually measuring the voltage of one HV source terminal relative to the optical link power supply, not the ground reference voltage of the HV source. An active optically-isolated HV probe by C. A. Bleys is eligible for real floating voltage measurements since the probe uses optical fibers for conveying signal and batteries as the power supply.<sup>4</sup> However, the probe circuit rapidly drains the batteries so the batteries must be replaced frequently. Since the probe is placed near HV sources, battery replacement can be awkward and even an electric hazard. Also, this probe is built with a fixed measurement range and requires calibration before each measurement.

We report here a fully isolated HV probe that uses both optical fibers and ordinary solar cells to isolate earth ground and avoid ground loops. The probe uses a low-capacitance lab-constructed HV capacitor and a precise 100 nF low voltage capacitor to form a voltage divider. Several HV capacitors with different capacitance were built so that the probe measurement range can easily be changed by switching the HV capacitors. The probe is powered by normal laboratory ambient light and so has no batteries and no reference to earth ground. The probe is well shielded and so can be used in extremely noisy environments. The probe does not require frequent calibration thanks to its relatively low temperature sensitivity, and the calibration can be conducted using low voltage sources.

The HV probe has a DC-5 MHz bandwidth and a  $\leq 30$  V noise level when measuring a fast varying HV source of  $-6$  to 2 kV.

## II. PROBE DESIGN

The probe system consists of an radio-frequency interference (RFI)/electromagnetic interference (EMI)-shielded, solar cell-powered transmitter that converts the high voltage signal into an amplitude-modulated (AM) optical signal, two low-loss optical fibers that convey the AM signal and a trigger signal, and a battery-powered receiver that converts the AM optical signal to a low voltage signal for a data

<sup>a)</sup>xzhai@caltech.edu.

<sup>b)</sup>pbellan@its.caltech.edu.

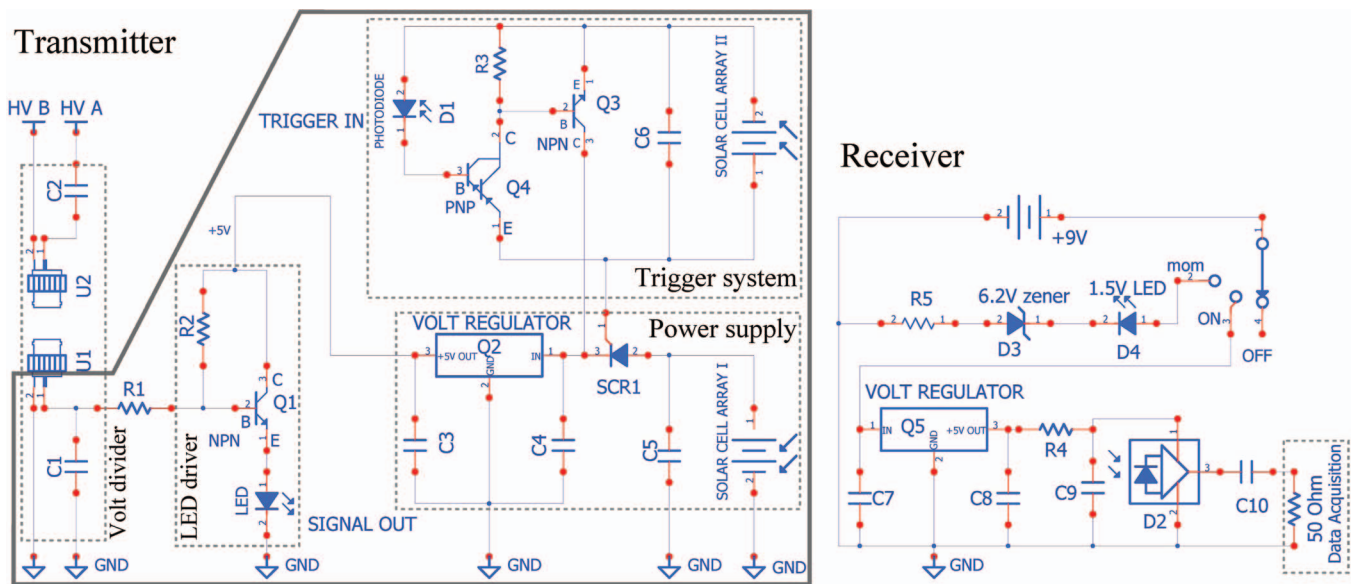


FIG. 1. Circuit diagram of the probe transmitter (left) and receiver (right). A typical configuration for the transmitter includes:  $C1 = 100$  nF (ECH-U1H104GX9 thin film; Panasonic Electronic Components),  $C2 = 60$  pF (lab-made),  $R1 = 20$  k $\Omega$ ,  $R2 = 7.5$  k $\Omega$ , Q1 NPN transistor (MMBT3904; Fairchild Semiconductor), LED (HFBR-1414 transmitter; Avago Technologies US Inc.), Q2 +5 V voltage regulator (LM340MP-5; National Semiconductor),  $C3 = 0.1$   $\mu$ F (ceramic bypass),  $C4 = 0.22$   $\mu$ F (ceramic bypass), SCR1 (S6X8BSRP; Littelfuse Inc.), Q3 NPN transistor (BC847CMTF; Fairchild Semiconductor), D1 PIN photodiode with ST mounting (OPF792; TT electronics/Optek Technology), Q4 PNP Darlington transistor (MMBTA64; Fairchild Semiconductor),  $R3 = 10$  k $\Omega$ ,  $C5 = 30$   $\mu$ F,  $C6 = 10$   $\mu$ F. The solar cell array I contains four mono-crystalline 33 mm  $\times$  37 mm solar cells (SCC3733-MSE; Solarbotics.com) in series; solar cell array II contains two same ones in series. Except  $C2$ , the entire circuit is enclosed in the 2" aluminum pipe (denoted by the thick solid polygon). The four dotted rectangles in the transmitter indicate the four transmitter subsystems. A typical configuration for the receiver includes: Q5 +5 V voltage regulator (LM340MP-5; National Semiconductor),  $C7 = 0.22$   $\mu$ F (ceramic bypass),  $C8 = 0.1$   $\mu$ F (ceramic bypass),  $R4 = 10$   $\Omega$ ,  $C9 = 33$  pF (ceramic bypass), D2 analog photodiode (HFBR-2416; Avago Technologies US Inc.),  $C10 = 47$   $\mu$ F (tantalum),  $R5 = 100$   $\Omega$ , D3 6.2 V zener diode (BZT52H-C6V2; NXP Semiconductors), D4 green LED (LTL-4236N; Lite-On Inc.), mom-off-on toggle switch (200MSP5T1B1M1QE; E-Switch).

acquisition device. The use of optical fibers allows the data acquisition device to be far from the HV source so that ordinary oscilloscopes or transient digitizers can be used to record data.

## A. Transmitter

The transmitter circuit diagram is shown in Fig. 1, and the figure caption lists the part numbers of the electronic components used in the circuit. The circuit contains four subsystems: a **capacitive voltage divider** that converts a high voltage to a low voltage, an **LED driver** that converts the low voltage signal to an AM optical signal, a **power supply**, and a **trigger system** that turns on the power supply immediately before measurements.

Except for the HV capacitor  $C2$ , the entire circuit, including the solar cells, is mounted on a single printed circuit board (PCB) and enclosed in a one-foot long 2" diameter aluminum pipe (Fig. 2). A female BNC adapter is mounted on the pipe end cap with its outer conductor connected to the pipe and the inner conductor connected to the junction point of  $C1$  and  $R1$  (see Fig. 1 for detail). In operation, the pipe is electrically connected to one electrode of the target HV source and constitutes the analog ground for the circuit. Four large apertures are milled in the pipe at the solar cell position and a steel mesh snugly covers these apertures. Light can thus shine on the solar cells inside the pipe, and yet the entire circuit is well shielded by the pipe and steel mesh.

## 1. Capacitive divider

$C2$  is a lab-constructed cylindrical HV capacitor. Figure 3 is a sketch for  $C2$ ; right and left hand here refer to this sketch.  $C2$  has two coaxial copper pipes (surface 2 and 4 in Fig. 3) with radii  $a$  and  $b$  ( $a < b$  and  $|b - a| \ll a$ ) as two electrodes and several layers of 0.254 mm-thick Mylar sheet in between as the dielectric (surface 3 in Fig. 3). The capacitance of  $C2$  is calculated by  $C2 \approx 2\pi aL\epsilon_0\epsilon_{eff}/d$ , where  $L$  is the overlap length of two copper pipes,  $d \equiv (b - a)$  and

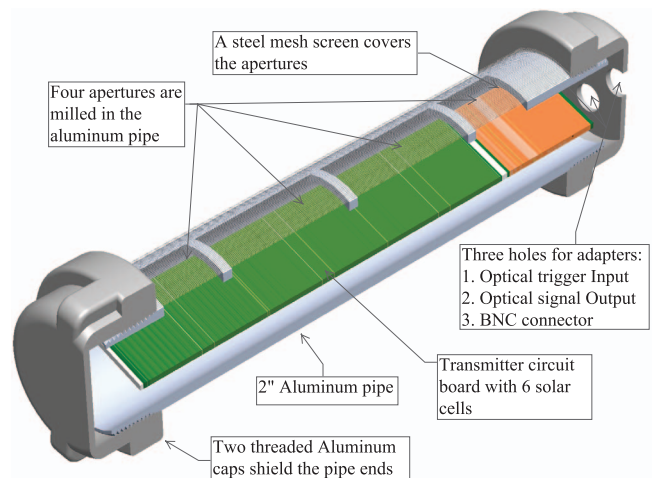


FIG. 2. Three dimensional cross section drawing of the transmitter without HV capacitor  $C2$ .

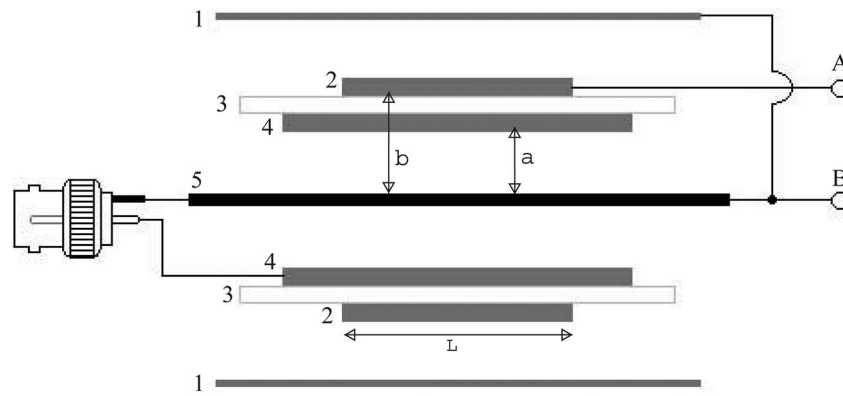


FIG. 3. Cross-sectional sketch of the lab-constructed cylindrical HV capacitor (C2 in Fig. 1). Five coaxial cylindrical surfaces/object are: (1) copper sheet, (2) outer copper pipe, (3) Mylar insulation and air gap, (4) inner copper pipe, (5) central HV wire. Terminal A and B are connected with HV sources terminals. A female BNC adapter's outer and inner conductors are connected to 5 and 4, respectively. The sketch is not to scale.

$\epsilon_{eff}$  is the effective relative dielectric constant of air ( $\epsilon_1 = 1$ ) and mylar sheets ( $\epsilon_2 \approx 3$ )<sup>4</sup> between the two copper pipes.  $\epsilon_{eff}$  is calculated by  $\epsilon_1 \epsilon_2 d / (d_1 \epsilon_2 + d_2 \epsilon_1)$ , where  $d_1$  and  $d_2 = d - d_1$  are the thickness of air and mylar, respectively. A typical HV capacitor has  $a = 1.44$  cm,  $b = 1.75$  cm,  $d = 3.1$  mm,  $L = 10$  cm, and  $d_2 = 2.54$  mm (10 layers mylar sheet). Hence,  $\epsilon_{eff} \approx 2.20$  and  $C2 \approx 60$  pF. Mylar has a dielectric strength 90 kV/mm.<sup>4</sup> Therefore, C2 can be safely charged to 10 kV or even higher. A 30 kV insulation high voltage wire (392275 WH005; Alpha Wire) is placed along the central axis of C2 (object 5 in Fig. 3). At the right hand end of C2, the central HV wire and the outer copper pipe connect with the two terminals A and B of the target HV source (see Fig. 3). At the left hand end of C2, the central HV wire and the inner copper pipe connect with the outer and inner conductor of a female BNC adapter, respectively.

To eliminate the possibility of capacitive coupling between C2 and any exterior charged surfaces, a copper sheet (surface 1 in Fig. 3) is wrapped around C2 and connected to the central HV wire.

A short RG58 coax cable links the HV capacitor's BNC adapter and the adapter on the aluminum pipe. By doing so, C2 and C1 inside the pipe form a capacitive voltage divider. Note that in this configuration, the common reference of the transmitter circuit and the aluminum pipe are electrically connected with the central HV wire through C2 and the electrode of the HV source that connects to the HV wire. Therefore, the entire transmitter uses the voltage of one HV source electrode as its reference voltage, and so the probe is completely floating relative to earth ground.

C1 is a fixed 100 nF thin film capacitor mounted on the PCB inside the aluminum pipe. The divided voltage by C1 and C2 equals  $C2 / (C1 + C2)$  times the high voltage, and is approximately  $C2 / C1$  if  $C1 \gg C2$ . Several versions of C2 are made with capacitance 20 pF, 40 pF, 60 pF, and so on. Because C2 is external and connected to the transmitter via a coax cable, it is easy to change C2 and therefore adjust the measurement range of the transmitter.

In the following discussion, we assume  $C2 = 60$  pF and the voltage of the HV source  $V_H$  is in the range of  $-6$  to 2 kV. Hence, the voltage across C1 is  $V_L = C2 / C1 \cdot V_H$  and

is in the range of  $-3.6$  to 1.2 V; the voltage across C2 is very nearly  $V_H$ .

## 2. LED driver

The divided low voltage  $V_L$  is converted into a current  $\Delta I$  by resistor R1.  $\Delta I$  modulates a constant bias current  $I_0$  flowing through R2 and then to the base of NPN transistor Q1. After being amplified  $\beta$  times by the transistor, this amplitude-modulated current is conducted into the fast HFBR-1414 light-emitting diode (LED). The LED sends an AM infrared signal into an optical fiber, which is then captured by the receiver. The resistors R1 and R2 are selected so that the LED works linearly when  $V_H$  is in the range of interest. At the same time,  $\tau \equiv R1 \times C1$  must be significantly greater than the measurement time to prevent loading of the voltage divider by the measuring circuit.

The power supply provides constant +5 V during measurements. The voltage at the transistor's base is about 2.3 V because of the forward voltage of Q1's base-emitter (BE) junction and the LED. Typically, we choose  $R1 = 20$  k $\Omega$  and  $R2 = 7.5$  k $\Omega$  so that the amplitude-modulated current  $\beta(I_0 + \Delta I)$  through the LED spans 13–60 mA, given the transistor's amplification factor  $\beta \approx 200$ . The current range 13–60 mA is located within the linear range 10–70 mA of the HFBR-1414 LED. For measurement time much less than  $\tau = 20$  k $\Omega \times 100$  nF = 2 ms, the voltage divider will not be significantly loaded by the LED driver during measurement.

## 3. Power supply

A capacitor (C5) charged by an array of solar cells (solar cell array I) with a voltage regulator (Q2) provides a constant +5 V for several milliseconds after being activated by the trigger system.

The solar cell array I shown in Fig. 1 contains four solar cells in series. Under normal lab ambient light, each solar cell unit can output  $\sim 30$   $\mu$ A at  $\sim 4$  V when inside the pipe. Therefore, solar cell array I can charge the 30  $\mu$ F capacitor C5 to  $\sim 15$  V in about 15 s. After the silicon controlled rectifier

(SCR)1 is switched on by the trigger system, C5 constitutes a short duration power source for voltage regulator Q2. The latter outputs a constant +5 V to the LED driver for  $\gtrsim 3$  ms (i.e., much longer than the measurement time  $50 \mu\text{s}$ ) until the pre-stored charge of C5 is drained. Then the SCR1 turns itself off automatically.

This power supply system allows the HV probe to perform a millisecond duration measurement every 15 s.

#### 4. Trigger system

Solar cell array I cannot power the LED directly because the LED requires at least 5 mA whereas Solar cell array I is capable of only  $30 \mu\text{A}$ . Therefore, SCR1 located at the output lead of capacitor C5 allows C5 to become fully charged. When SCR1 is in the off state, the probe is inactive and solar cell array I charges C5 to  $\sim 15$  V. SCR1 is switched on by the trigger system just before measurements. The trigger system is powered by a separate solar cell array II.

A 175 MHz pin photodiode D1 (OPF792, see Fig. 1) is used to receive an externally generated optical trigger signal. D1 has a typical dark current 0.1–0.5 nA and outputs current  $\geq 20$  nA when triggered by an optical signal. A PNP transistor Q4 amplifies the current by a factor of  $10^4$ . R3 is selected to be  $10 \text{ k}\Omega$  so that its voltage exceeds 0.7 V only when D1 is triggered. Since R3 is parallel to the BE junction of a NPN transistor Q3, Q3 then switches on because its BE voltage exceeds 0.7 V. Therefore, the fully charged capacitor C6 is switched across the gate-cathode junction of SCR1, which turns on in  $\sim 2 \mu\text{s}$ . The entire trigger system including SCR1 takes  $\approx 3 \mu\text{s}$  to activate the voltage regulator Q2 after receiving the optical trigger signal. Therefore, the external trigger signal must be sent to D1 at least  $3 \mu\text{s}$  before measurements.

The dark current of the trigger system is only  $\leq 0.5 \text{ nA} \times 10^4 = 5 \mu\text{A}$ . Therefore, an ordinary solar cell is fully capable to serve as a power supply for the system under normal lab ambient light. To have the trigger system working reliably, the output voltage of solar cell II must be at least 1.5 V to turn on the Darlington PNP transistor Q4. In a typical configuration, two solar cell units in series form the solar cell array II (see Fig. 1).

#### B. Receiver

The receiver of the HV probe converts the AM optical signal sent by the transmitter into a voltage signal. Its circuit diagram is shown in Fig. 1, essentially an analog HFBR-2416 photodiode receiver. The part numbers are listed in the figure caption. HFBR-2416 outputs an analog voltage signal proportional to the AM optical signal. A voltage regulator Q5 powered by a +9 V battery provides the HFBR-2416 photodiode with constant +5 V. A battery test can be done by switching the toggle to momentary position 2. The capacitor C10 between HFBR-2416 and  $50 \Omega$  data acquisition device adds an AC coupling to the voltage signal output. Its capacitance is  $47 \mu\text{F}$  so that  $47 \mu\text{F} \times 50 \Omega = 2.35 \text{ ms} \gg 50 \mu\text{s}$ , the measurement time.

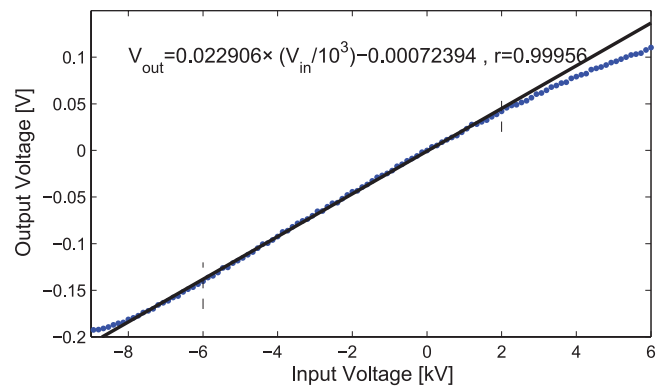


FIG. 4. HV probe calibration result with C2 = 60 pF. The solid line gives the least-square fit to the experimental data (dotted curve) in  $-6$  to  $2$  kV.

With the HV source measuring the range  $-6$  to  $2$  kV and the driving current in the range of  $10$  to  $60$  mA for the HFBR-1414 LED, the receiver outputs a proportional voltage signal of  $-0.15$  to  $0.05$  V (see subsection II C.).

The optical fibers totally isolate the transmitter and the high voltage source, and so allow long-distance remote measurement. Meanwhile, the receiver can be safely connected to data acquisition devices directly, such as transient digitizers or oscilloscopes.

#### C. Calibration

Knowing the capacitance of C1 and C2, one can use a low voltage source to calibrate the probe without utilizing a high voltage source standard. The calibration to the HV probe can be conveniently done by disconnecting the HV capacitor C2 and connecting a low voltage function generator to the BNC adapter on the aluminum pipe. By doing so, we are applying the low voltage directly to the junction point of the capacitive divider.

For example, we apply a  $50 \text{ kHz} \pm 10 \text{ V}$  sine function to the junction point using a WAVETEK model 143 function generator and measure the receiver output using a Tektronix TDS1002 oscilloscope. After calculating the divided voltage in-out gain  $V_{junc}/V_{out}$ , the total gain  $V_{in}/V_{out}$  is obtained by multiplying it with  $(C1 + C2)/C2$ , where  $C1 = 100 \text{ nF}$  and  $C2$  is measured to be  $60 \text{ pF}$  using a BK PRECISION model 885 LCR/ESR meter. Figure 4 shows the calibration result and verifies the linearity of the probe over the range from  $-6$  to  $2$  kV.

### III. PERFORMANCE AND MEASUREMENT

Figure 5 shows a typical measurement of a pulsed power plasma experiment<sup>5–8</sup> that produces a magnetohydrodynamic plasma loop. The plasma is formed by charging a  $60 \mu\text{F}$  capacitor to  $-3$  kV and discharging it across a neutral Hydrogen gas for  $\approx 10$ – $20 \mu\text{s}$ . The well-defined plasma loop lasts about  $5$ – $10 \mu\text{s}$  and then exhibits complex dynamic behaviors. The entire voltage/current profile lasts about  $50 \mu\text{s}$  during which the voltage across the electrodes swings between  $\pm 3$  kV and the current through the electrodes oscillates over  $\pm 35$  kA.

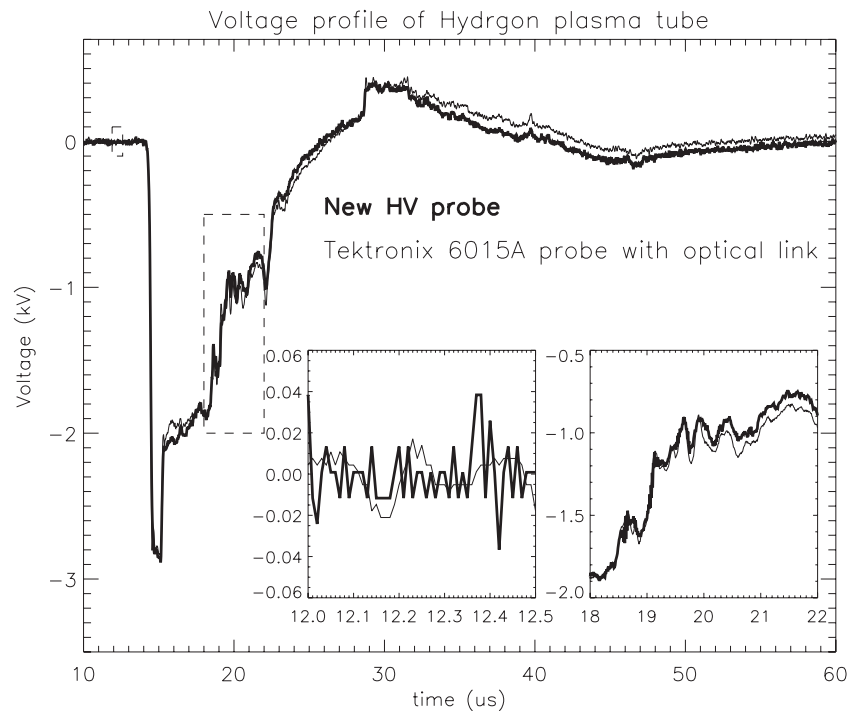


FIG. 5. Voltage across a pulse powered Hydrogen plasma measured by the new HV probe (the heavy curve) and a Tektronix P6015A HV probe (the light curve). Two boxes at right lower corner zoom into the time interval 12–12.5  $\mu\text{s}$  and 18–22  $\mu\text{s}$ , showing the detailed behavior of the voltage profile. The high voltage is applied at 14.5  $\mu\text{s}$ . The two measurement curves are unsmoothed raw data multiplied by the corresponding calibration factors. Shot number = 9950.

The total power of the plasma can reach  $\geq 100$  MW. The measurement by the HV probe described by this paper (stated as the new HV probe in the following content) is compared with the measurement by a Tektronix P6015A 75MHz probe that has been properly compensated. A DC-10MHz analog fiber optic link (732T/R; Analog Modules Inc.) is used to convey the Tektronix probe output to the data acquisition device and break the ground loop. The power supply for the optical link is isolated from earth by a transformer. The new HV probe is calibrated using the method presented in Sec. II. The HV wire and the outer copper pipe in C2 are connected to the anode and cathode of the plasma gun, respectively. A 12-Bit 100 MHz VMEbus digitizer (SIS3000, Struck Innovative Systeme) with a  $\pm 0.5$  V dynamic range is used for recording the data.

The detailed voltage profile from 12 to 12.5  $\mu\text{s}$  in the inserted in Fig. 5 demonstrates that the new HV probe has a white noise generally below 0.03 kV. Figure 5 shows that the new HV probe and the Tektronix probe agree with each other quite well over a 50  $\mu\text{s}$  long measurement. The discrepancy between the two probes is generally  $\leq 0.05$  kV. They both capture fast voltage fluctuations as short as  $\sim 0.2$   $\mu\text{s}$  (see insert in Fig. 5 from 18 to 22  $\mu\text{s}$ ).

The NPN transistor Q1, the HFBR-1414 LED, and the HFBR-2416 photodiode used in the probe are all high-speed devices with bandwidth  $\geq 100$  MHz. The bandwidth of the probe is determined by the low-pass filter formed by R1 and the BE junction of Q1. The RC time of this low-pass filter is  $\approx 20$  k $\Omega \times 2.5$  pF  $\sim 50$  ns, resulting in a  $\sim 90$  ns rise time for the entire HV probe. Although this is sufficient for the  $\leq 50$   $\mu\text{s}$  long voltage measurements, the bandwidth of the

probe could be improved by using a smaller R1, say, 3 k $\Omega$  ( $R1 \times C1 = 300$   $\mu\text{s} \gg 50$   $\mu\text{s}$  is still satisfied). However, this will change the probe sensitivity. Alternatively, the probe could have a wider bandwidth by replacing Q1 by a high speed transistor with sub-pF BE capacitance. A rise time as short as 15 ns should then be achievable using the same LED and photodiode.

The HFBR-2416 photodiode in the receiver is responsible for most of the noise. The unfiltered RMS output noise of the photodiode is  $\leq 0.6$  mV, corresponding to an input voltage  $\leq 0.025$  kV assuming system gain 0.0229 V/kV. The digitization rounding error of SIS3000 is  $1/2^{12}$  V = 0.25 mV, corresponding to a 0.01 kV input voltage. The combination of the two noise sources gives  $\sim 0.03$  kV, consistent with Fig. 5. The power of the output noise is only  $\leq (0.7$  mV) $^2/50$   $\Omega \sim 10$  nW, which is  $\leq 10^{-16}$  times of the total power of the pulsed power plasma.

The system has a temperature dependence of  $\approx 1.5\%/C^\circ$  at room temperature in  $V_{out}/V_{in}$  gain, mostly contributed by the HFBR-1414 LED in the transmitter. The heat generated by the circuit is negligible since each measurement lasts for milliseconds. However, the probe should be recalibrated if the ambient temperature has varied significantly.

In conclusion, we have reported an ambient light powered wideband optically-coupled floating-input active HV probe. Because of its excellent EMI/RFI shielding, the HV probe is useful for the precise measurement of pulsed high voltages over a DC–5MHz bandwidth in a noisy environment. Due to the special connection design for the capacitive divider, the HV probe has an adjustable measurement range and is easy to calibrate.

## ACKNOWLEDGMENTS

The authors thank D. D. Felt for his suggestion on the trigger system. This work was supported by the U.S. Department of Energy (DOE).

<sup>1</sup>W. J. Sarjeant and A. J. Alcock, *Rev. Sci. Instrum.* **47**, 1283 (1976).

<sup>2</sup>R. Gratton, S. Mangioni, J. Niedbalski, and R. Valent, *Rev. Sci. Instrum.* **57**, 2634 (1986).

<sup>3</sup>S. H. Saw, C. S. Wong, and S. Lee, *Rev. Sci. Instrum.* **62**, 532 (1991).

<sup>4</sup>C. A. Bleys, *Rev. Sci. Instrum.* **47**, 621 (1976).

<sup>5</sup>J. F. Hansen, S. K. P. Tripathi, and P. M. Bellan, *Phys. Plasmas* **11**, 3177 (2004).

<sup>6</sup>D. Kumar and P. M. Bellan, *Phys. Rev. Lett.* **103**, 105003 (2009).

<sup>7</sup>S. C. Hsu and P. M. Bellan, *Phys. Plasmas* **12**, 032103 (2005).

<sup>8</sup>D. Kumar, A. Moser, and P. Bellan, *IEEE Trans. Plasma Sci.* **38**, 47 (2010).